C55.13: NESS 61

A UNITED STATES DEPARTMENT OF COMMERCE PUBLICATION

NOAA Technical Report NESS 61

U.S. DEPARTMENT OF COMMERCE
National Oceanic and Atmospheric Administration
National Environmental Satellite Service

The Measurement of Atmospheric Transmittance From Sun and Sky With an Infrared Vertical Sounder

PENNSYLVANIA STATE UNIVERSITY
NOV

W. L. SMITH AND H. B. HOWELL

WASHINGTON, D.C.
September 1972

NOAA TECHNICAL REPORTS

National Environmental Satellite Service Series

The National Environmental Satellite Service (NESS) is responsible for the establishment and operation of the National Operational Meteorological Satellite System and of the environmental satellite systems of NOAA. The three principal Offices of NESS are Operations, Systems Engineering, and Research. The NOAA Technical Report NESS series is used by these Offices to facilitate early distribution of research results, data handling procedures, systems analyses, and other information of interest to NOAA organizations.

Publication of a Report in NOAA Technical Report NESS series will not preclude later publication in an expanded or modified form in scientific journals. NESS series of NOAA Technical Reports is a continuation of, and retains the consecutive numbering sequence of, the former series, ESSA Technical Report National Environmental Satellite Center (NESC), and of the earlier series, Weather Bureau Meteorological Satellite Laboratory (MSL) Report. Reports 1 to 57 are listed in publication NESC 56 of this series.

Reports 1 to 50 in the series are available from the National Technical Information Service, U.S. Department of Commerce, Sills Bldg., 5285 Port Royal Road, Springfield, Va. 22151. Price: $3.00 paper copy; $0.95 microfiche. Order by accession number, when given, at end of each entry. Beginning with 51, Reports are available through the Superintendent of Documents, U.S. Government Printing Office, Washington, D.C. 20402.

ESSA Technical Reports

NESC 38. Angular Distribution of Solar Radiation Reflected from Clouds as Determined from TIROS IV Radiometer Measurements, I. Ruff, R. Koffler, S. Fritz, J. S. Winston, and P. K. Rao, March 1967. (PB 174 729)

NESC 39. Motions in the Upper Troposphere as Revealed by Satellite Observed Cirrus Formation, H. McClure Johnson, October 1966. (PB 173 996)

NESC 40. Cloud Measurements Using Aircraft Time-Lapse Photography, L. F. Whitney, Jr., and E. Paul McClain, April 1967. (PB 174 728)

NESC 41. The SINAP Problem: Present Status and Future Prospects. Proceedings of a Conference held at the National Environmental Satellite Center, Suitland, Md., January 18-20, 1967, E. Paul McClain, Reporter, October 1967. (PB 176 570)

NESC 42. Operational Processing of Low Resolution Infrared (LRIR) Data from ESSA Satellites, Louis Rubin, February 1968. (PB 178 123)

NESC 43. Atlas of World Maps of Long-Wave Radiation and Albedo -- For Seasons and Months Based on Measurements from TIROS IV and TIROS VII, J. S. Winston and V. Ray Taylor, September 1967. (PB 176 569)

NESC 44. Processing and Display Experiments Using Digitized ATS-1 Spin Scan Camera Data, M. B. Whitney, R. C. Doolittle, and B. Goddard, April 1968. (PB 178 424)

NESC 45. The Nature of Intermediate-Scale Cloud Spirals, Linwood F. Whitney, Jr., and Leroy D. Herman, May 1968. (AD-673 681)

NESC 46. Monthly and Seasonal Mean Global Charts of Brightness From ESSA 3 and ESSA 5 Digitized Pictures, February 1967-February 1968, V. Ray Taylor and Jay S. Winston, November 1968. (PB 180 717)

NESC 47. A Polynomial Representation of Carbon Dioxide and Water Vapor Transmission, William L. Smith, February 1969. (PB-183 296)

NESC 48. Statistical Estimation of the Atmosphere's Geopotential Height Distribution From Satellite Radiation Measurements, William L. Smith, February 1969. (PB 183 297)

NESC 49. Synoptic/Dynamic Diagnosis of a Developing Low-Level Cyclone and Its Satellite-Viewed Cloud Patterns, Harold J. Brodrick and E. Paul McClain, May 1969. (PB 184 612)

NESC 50. Estimating Maximum Wind Speed of Tropical Storms from High Resolution Infrared Data, L. F. Hubert, A. Timchalk, and S. Fritz, May 1969. (PB 184 611)

NESC 51. Application of Meteorological Satellite Data in Analysis and Forecasting, R. K. Anderson, J. P. Ashman, F. Bittner, G. R. Farr, E. W. Ferguson, V. J. Oliver, and A. H. Smith, September 1969. (AD-697 033)

NESC 52. Data Reduction Processes for Spinning Flat-Plate Satellite-Borne Radiometers, Torrence H. MacDonald, July 1970.

NESC 53. Archiving and Climatological Applications of Meteorological Satellite Data, John A. Leese, Arthur L. Booth, and Frederick A. Godshall, July 1970. (COM-71-00076)

NESC 54. Estimating Cloud Amount and Height From Satellite Infrared Radiation Data, P. Krishna Rao, July 1970. (PB-194 685)

NESC 56. Time Longitude Sections of Tropical Cloudiness (December 1966-November 1967), J. M. Wallace, July 1970.

NOAA Technical Reports

NESS 55. The Use of Satellite-Observed Cloud Patterns in Northern Hemisphere 500-mb Numerical Analysis, Roland E. Nagle and Christopher M. Hayden. April 1971.

(Continued inside back cover)

U.S. DEPARTMENT OF COMMERCE
Peter G. Peterson, Secretary

NATIONAL OCEANIC AND ATMOSPHERIC ADMINISTRATION
Robert M. White, Administrator

NATIONAL ENVIRONMENTAL SATELLITE SERVICE
David S. Johnson, Director

NOAA Technical Report NESS 61

The Measurement of Atmospheric Transmittance From Sun and Sky With an Infrared Vertical Sounder

W. L. Smith and H. B. Howell

WASHINGTON, D.C.
SEPTEMBER 1972

U. S. Depository Copy

For sale by the Superintendent of Documents, U.S. Government Printing Office, Washington, D.C. 20402. Price 30 cents.

UDC 551.501.721:551.508.21:551.521.3:535-1

551.5 Meteorology
.501 Methods of observation
.721 Radiation observation
.508 Instruments
.21 Radiometers
.521 Radiation
.3 Transmittance in atmosphere
535-1 Infrared radiation

CONTENTS

Abstract. 1

1. Introduction. 1

2. The ITPR instrument 1

3. Transmittance determination 2

A. From solar radiances. 2

B. From sky radiances. 3

C. The Mauna Loa experimental set-up and measurement technique . . . 4

D. Supporting conventional observations. 7

E. The theoretical transmittance model 10

4. Results of the Mauna Loa observations 10

5. Conclusion and additional considerations. 12

Acknowledgments. 15

References. 16

Digitized by the Internet Archive
in 2013

http://archive.org/details/measurementofatm00smit

THE MEASUREMENT OF ATMOSPHERIC TRANSMITTANCE FROM SUN AND SKY WITH AN INFRARED VERTICAL SOUNDER*

W. L. Smith and H. B. Howell
National Environmental Satellite Service
National Oceanic and Atmospheric Administration
Washington, D. C.

ABSTRACT. This paper describes the determination of atmospheric transmittance from ground-based sun and sky radiance measurements with a prototype of the Nimbus E Infrared Temperature Profile Radiometer (ITPR).

1. INTRODUCTION

The direct inference of vertical temperature and moisture profiles from spectral radiance observations requires precise knowledge of the atmospheric transmission properties of the atmosphere. The atmospheric transmission functions used in the numerical solution for atmospheric structure are usually modelled by using data obtained from laboratory measurements or by theoretical computation. Experience has shown that, to make meteorological inferences with the required accuracy from remote radiance observations, empirical corrections must usually be made.

For spectral regions where molecular scattering is negligible, empirical determinations of atmospheric transmittance can be made from solar radiance and sky-emission radiance measurements. Such measurements, made at various altitudes and viewing angles, can be used to derive the dependence of transmittance on pressure, temperature, and gas concentration.

This paper describes the determination of atmospheric transmittance from ground based sun and sky radiance measurements with a prototype of the Nimbus E Infrared Temperature Profile Radiometer (ITPR). The observations were obtained during November and December of 1971 from altitude 11,150 feet at the Mauna Loa Observatory, Hawaii. The measurements were conducted to check, and to correct as necessary, transmission models formulated from theoretical line-by-line calculations for application to the spacecraft ITPR measurements.

2. THE ITPR INSTRUMENT

The ITPR is a seven-channel sounding radiometer that measures radiance in the 3.7-μm and 11-μm "atmospheric windows", in four different portions of the 15-μm CO_2 band, and in an interval near 20μm in the rotational water vapor band. Spectral definition is accomplished using narrow-band interference filters. The spectral response functions for the ITPR are presented in figure 1. Its effective uniform response viewing aperture is 3.57×10^{-4} steradians.

*Presented at the International Radiation Symposium (IAMAP/IUGG), Sendai, Japan, May 26 - June 2, 1972.

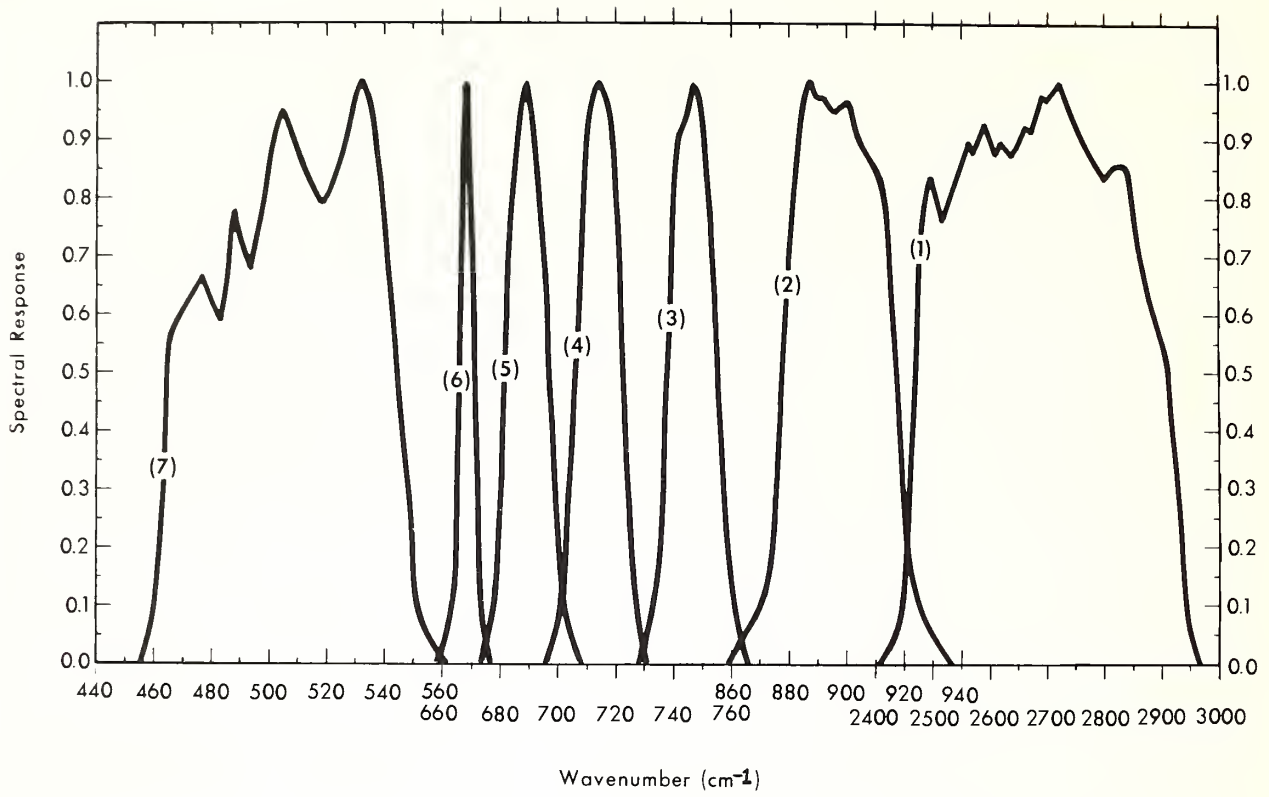

Figure 1.--Spectral response functions for the seven ITPR channels.

3. TRANSMITTANCE DETERMINATION

A. From Solar Radiances

The transmittance of the atmosphere can be specified from the radiances measured when viewing, in turn, the solar disc and the sky away from the solar disc, using the relation

$$\tau(\theta) = \frac{I_s(\theta) - I_a(\theta)}{I_o} \qquad (1)$$

where $\tau(\theta)$ is the transmittance of the atmosphere along the direction θ, $I_s(\theta)$ is the radiance from the sun and the intervening atmosphere measured by viewing towards the sun, $I_a(\theta)$ is the radiance from only the atmosphere measured by viewing away from the sun, and I_o is the effective solar radiance at the top of the atmosphere. The term "effective" is used here to indicate that I_o is the radiance of an extended blackbody source filling the instrument's aperture, which would produce the same response as viewing the solar disc from the top of the atmosphere. From a mountain platform, the transmittance is obtained as a function of gas concentration by observing the sun at various solar elevation angles.

The effective solar radiance for each ITPR channel was computed from the

solar brightness temperatures obtained from the solar radiance values given by Thekaekara, Drummond et al. (1971). Table 1 summarizes these brightness temperatures, the corresponding Planck radiances, and the average radiances across the instrument's field of view which would be sensed by viewing the sun through a completely transparent atmosphere at Mauna Loa in December (i.e., the solid angle of 7.0×10^{-5} steradians subtended by the sun).

Table 1.--Solar brightness temperature, solar radiance, effective solar radiance, and effective solar brightness temperature

Channel	Central wavenumber (cm^{-1})	T_s (°K)	I_s($mw/m^2.sr.cm^{-1}$)	I_o($mw/m^2.sr.cm^{-1}$)	T_e (°K)
1	2679	5,798	242,460	47,541	2,210
2	899	5,046	29,562	5,796	1,435
3	747	4,945	20,477	4,015	1,354
4	714	4,245	15,881	3,114	1,194
5	690	4,245	14,881	2,918	1,183
6	668	4,869	16,332	3,202	1,307
7	507	4,897	9,948	1,951	1,265

B. From Sky Radiances

The transmittance of the atmosphere can be derived from measurements of sky emission if the temperature and absorbing gas profiles are known. Given an a priori estimate of the transmittance profile of the atmosphere obtained from a theoretical model, the actual transmittance profile is assumed to be given by

$$\ln\left[-\ln\tau(p,\theta)\right] = \ln\left[-\ln\hat{\tau}(p,\theta)\right] + k_o + k_1 \ln U(p,\theta) \qquad (2)$$

where $\tau(p, \theta)$ is the true transmittance profile as a function of pressure p along the viewed direction θ, $\hat{\tau}(p,\theta)$ is the transmittance profile given by the theoretical model, and $U(p,\theta)$ is the absorbing gas concentration profile. The constants k_o and k_1 are parameters that account for the errors of the physical characteristics of the model; k_o accounts for the error of the logarithm of the absorption coefficient and k_1 accounts for the error of the way in which transmittance in the model depends on gas concentration.

Equation (2) states that

$$\tau(p,\theta) = \hat{\tau}(p,\theta)^{\alpha(p,\theta)} \tag{3}$$

with

$$\alpha(p,\theta) = \left[U(p,\theta)\right]^{k_1} e^{k_o}$$

The error coefficients k_o and k_1 can be related to the measured sky radiance and that radiance calculated with a theoretical model using the differential equation:

$$dI(\theta) = \left[\frac{\partial I(k_o,0,\theta)}{\partial k_o}\right] dk_o + \left[\frac{\partial I(0,k_1,\theta)}{\partial k_1}\right] dk_1 \tag{4}$$

where $I(k_o,0,\theta)$ is the radiance computed as a function of k_o using the modification of the theoretical transmittance given by (3) for $k_1 = 0$, while $I(0,k_1,\theta)$ is that radiance computed as a function of k_1 for $k_o = 0$. For an upward-viewing instrument the radiative transfer equation relating the emitted sky radiance to the transmission profile is

$$I(\theta) = \int_{P_o}^{o} B\left[T(p)\right] \frac{d\tau(p,\theta)}{dp}\, dp \ , \tag{5}$$

where $B\left[T(p)\right]$ is the effective Planck radiance profile for the spectral interval of measurement given by the temperature profile $T(p)$.

In this study, the error coefficients k_o and k_1 are determined from radiance measurements and calculated radiance values for four zenith angles (Sec θ = 1, 2, 4, and 8) through the solution of the set of four simultaneous equations given by the numerical form of (4);

$$I(\theta_i) - I(0,0,\theta_i) = \left\{\frac{I(0.25,0,\theta_i) - I(-0.25,0,\theta_i)}{0.5}\right\} k_o + \left\{\frac{I(0,0.25,\theta_i) - I(0,-0.25,\theta_i)}{0.5}\right\} k_1 \tag{6}$$

where $I(\theta_i)$ is sky emission measured at angle θ (for Sec θ_i =1, 2, 4, 8) and $I(0,0,\theta)$ is the radiance computed using the theoretical transmission model (i.e., $k_o = k_1 = 0$). The transmission profiles for initial and resultant values of k_o and k_1 are computed using (3).

For spectral channels where both CO_2 and H_2O absorb, the k_o and k_1 for CO_2, the major constituent, were determined by assuming that the total transmittance is given by the product of the empirical CO_2 transmittance and the theoretical H_2O transmittance.

C. The Mauna Loa Experimental Set-Up and Measurement Technique

The ITPR, mounted on a precision rotary table, could be leveled to within 1 minute of arc. Figure 2 is a block diagram of the experimental configuration. The entire apparatus, including the optical and electronic units,

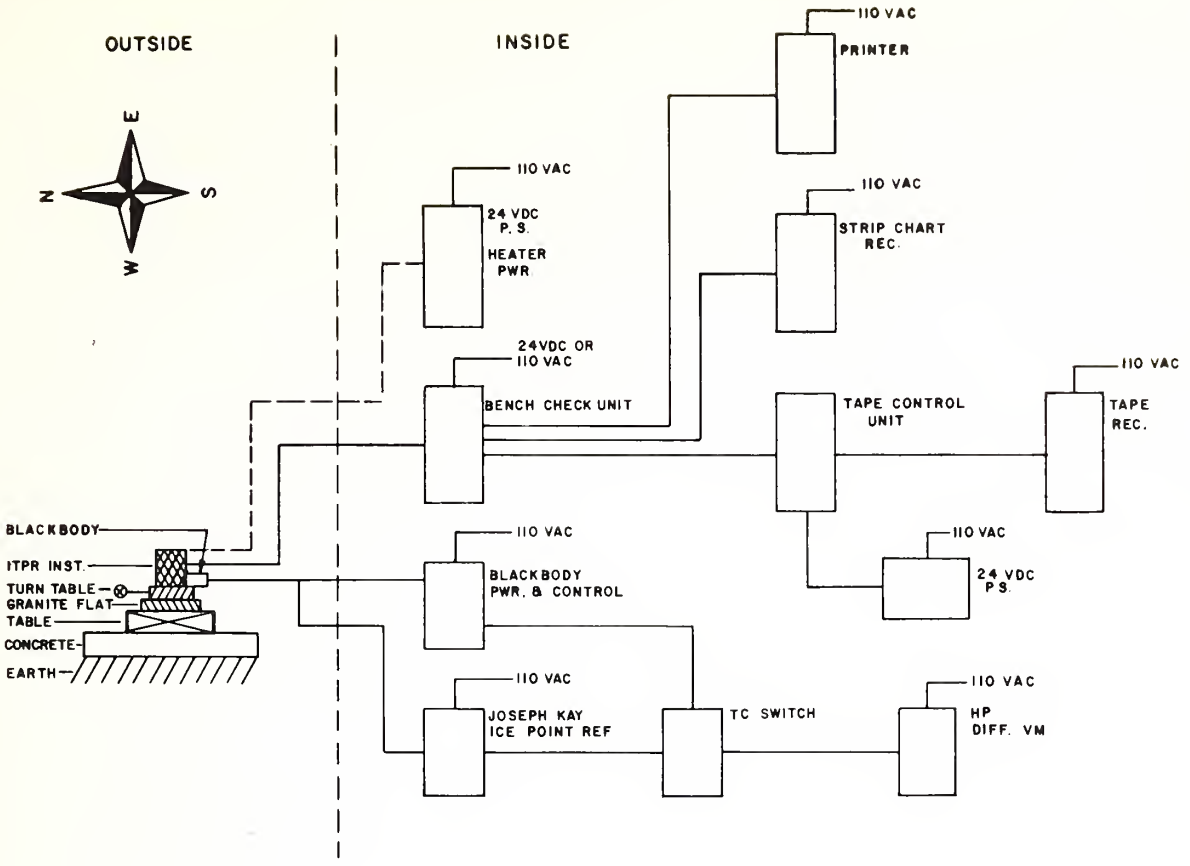

Figure 2.--Block diagram of the ITPR Mauna Loa experiment.

A-to-D converter, calibration blackbody assembly, and digital output display and printer devices were located on an observation platform that permitted unrestricted viewing of the solar disc from sunrise to sunset.

The local zenith angle pertaining to a particular sun measurement is defined for the instrument location (latitude, longitude) by the time at which a maximum radiance was observed as the sun crossed the field of view of the instrument. The scan mirror was set at an angle corresponding to the predicted solar elevation. Small adjustments in azimuth were made during the observation period to place the solar image in the most responsive portion of the field of view. As soon as the maximum radiance was encountered, the instrument was rotated about 10° in azimuth to obtain a measurement of the sky radiance alone. The difference of the radiances obtained by viewing first the solar disc and then the clear sky provided the measure of solar radiance transmitted through the atmosphere along the path of view. The solar radiances measured during several cloudfree days at the Mauna Loa Observatory are presented in figure 3.

Independent sky emission measurements were also obtained by scanning from local vertical to the horizon over a period of several minutes. In this case the elevation angle of the measurement was determined from the angle of the scan mirror, which is accurate to within less than 1 minute of arc. Small errors introduced by the uncertainty in the orientation of the scan mirror and the instrument baseplate were alleviated by rotating the instrument 180°

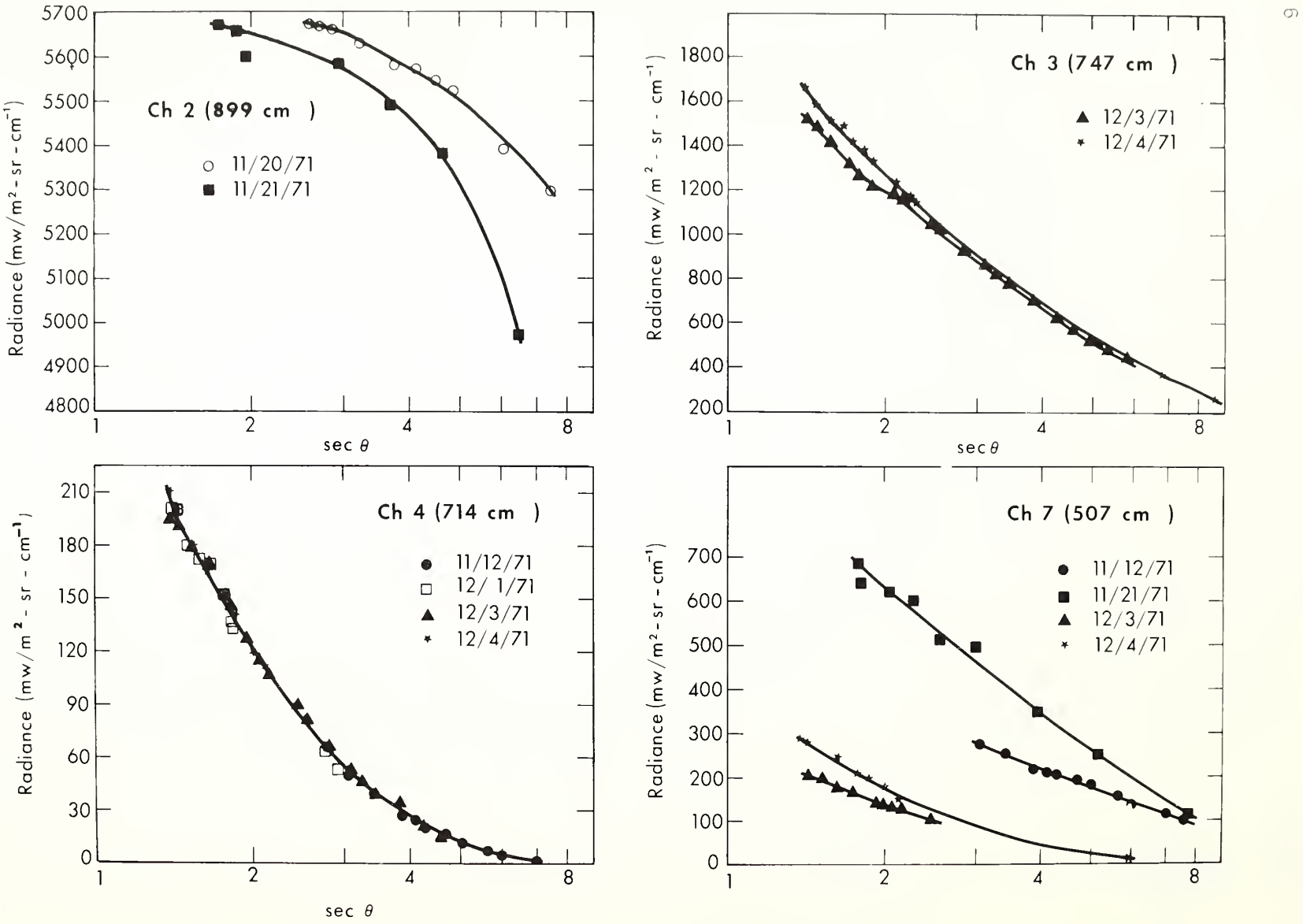

Figure 3.--Solar radiances measured by ITPR channels 2, 3, 4, and 7 during November and December 1971.

and repeating the angular scan by viewing the same atmosphere through the opposite side of the viewing cavity. The average of the two scans provided sky emission radiance as a function of the absolute viewing angle. The radiances obtained in this manner are shown in figure 4.

Measurements of solar and sky radiance are not shown for channels 1, 5, and 6. Channel 1 solar radiances could not be observed because the intense incoming energy could not be attenuated adequately or reliably. Useful emission data for channel 1 could not be obtained because the radiances measured when viewing cold space through the atmosphere were close to the channel noise level (0.006 $mw/m^2 \cdot sr \cdot cm^{-1}$). Channels 5 and 6, which are situated in relatively intense portions of the 15-μm CO_2 absorption band, did not provide useful sky emission data since the atmosphere is opaque to radiation measured in these channels.

D. Supporting Conventional Observations

Special vertical temperature and moisture profile measurements were made by radiosonde from the Hilo Weather Station during each radiometric observation period. The portions of these profiles that were above the pressure altitude of the Mauna Loa Observatory (680 mb) are illustrated in figure 5.

Surface observations were also obtained from continuous recorders at the observatory. The average values of surface temperature and water vapor mixing ratio adopted for each radiometric observation period are presented in table 2.

Table 2.--Surface temperature and water vapor mixing ratio observations, total water vapor concentration, and radiosonde "tie-on" level

Date	Temperature (°C)	Mixing ratio (g/kg)	Total water vapor concentration (pr.cm.)*	Radiosonde tie on level (mb)
Nov. 12, 1971	13.4	6.8	0.229	676
Nov. 20, 1971	12.4	5.2	0.134	676
Nov. 21, 1971	12.8	5.3	0.177	679
Nov. 22, 1971	11.8	6.0	0.184	679
Dec. 1, 1971	11.5	7.2	0.544	677
Dec. 3, 1971	12.0	10.0	0.570	668
Dec. 4, 1971	12.1	10.5	0.544	677

*Precipitable centimeters

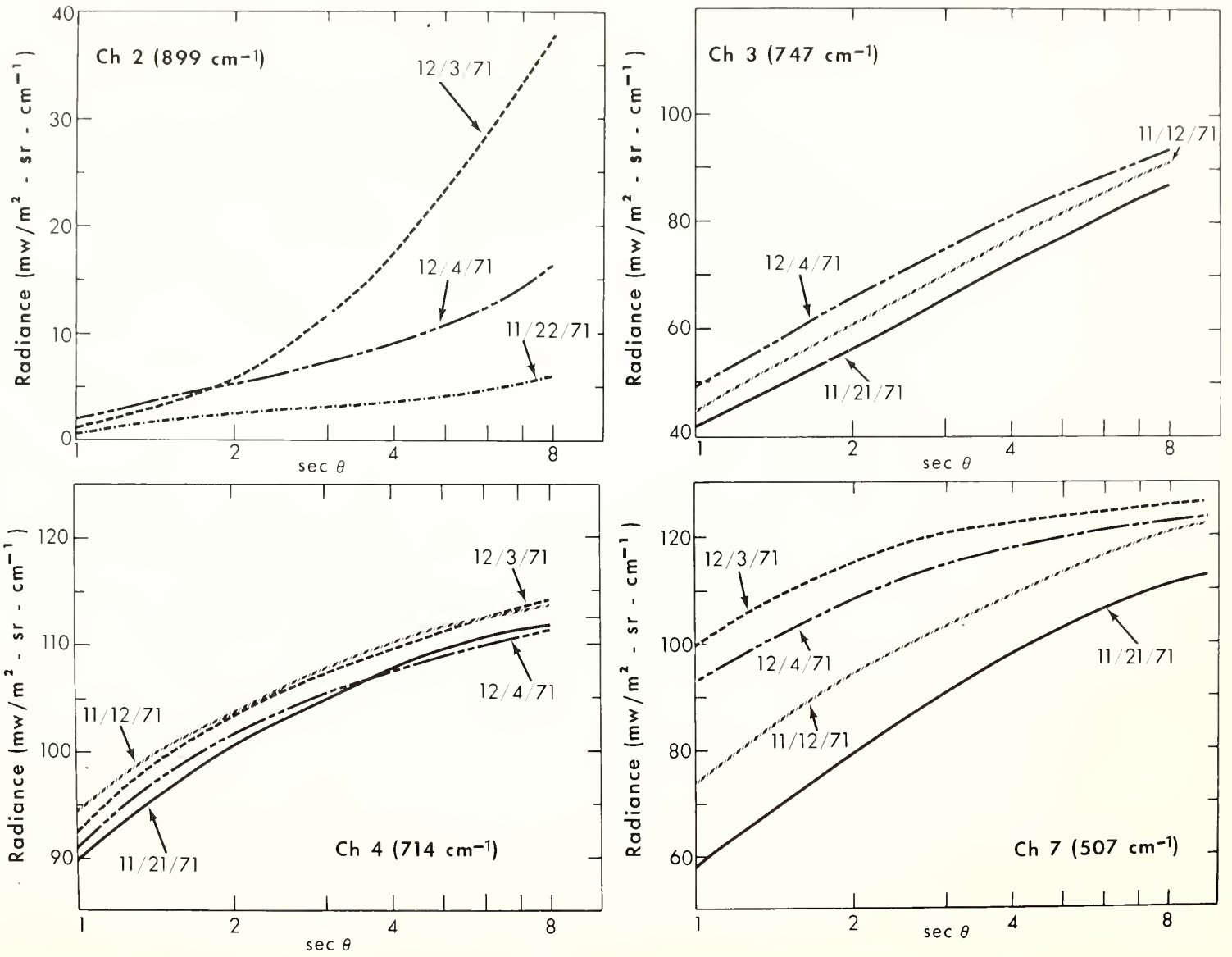

Figure 4.--Sky emission radiances measured by ITPR channels 2, 3, 4, and 7 during November and December 1971.

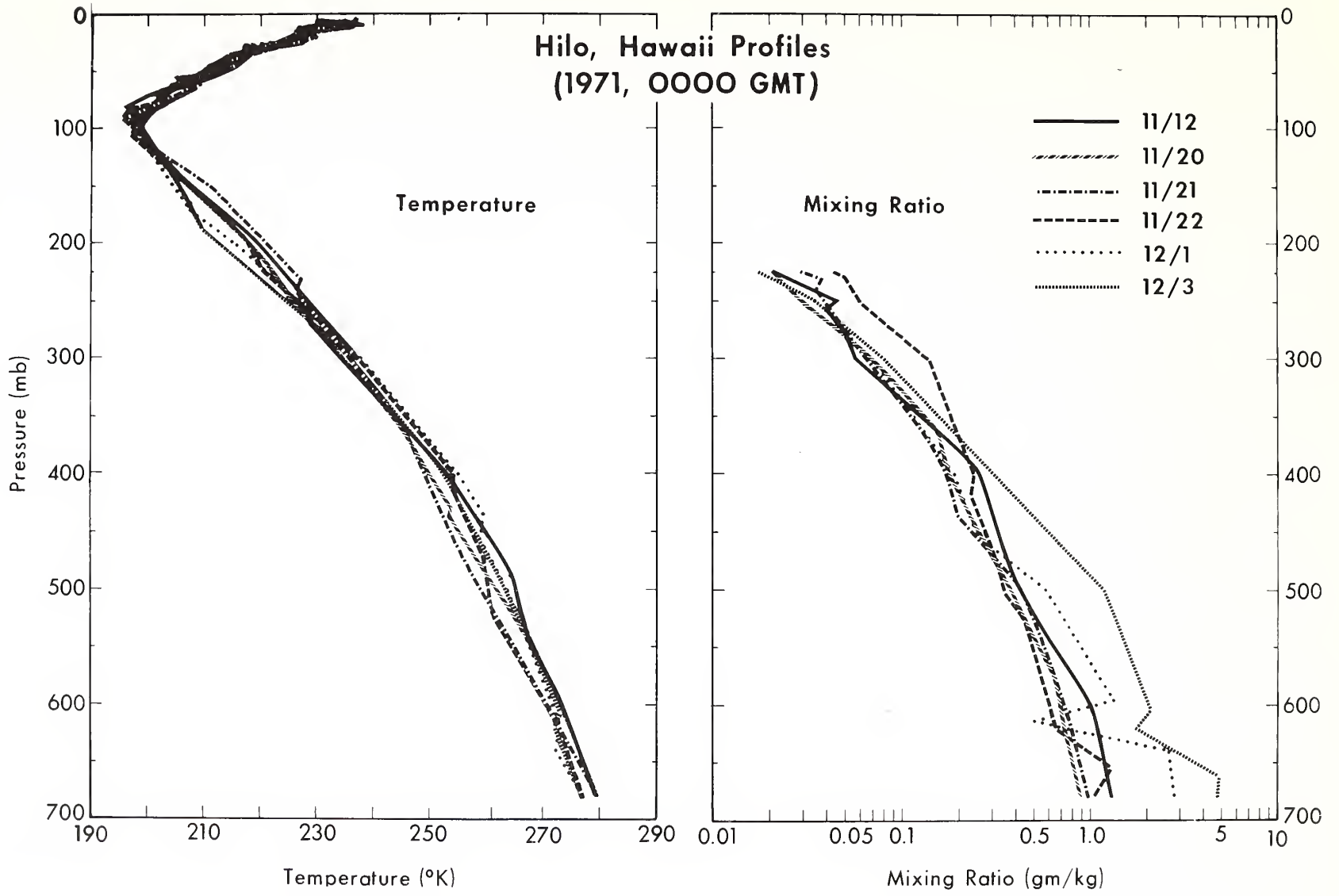

Figure 5.--Hilo, Hawaii, radiosonde-observed temperatures and mixing ratios for the radiance observation periods.

There usually are dramatic differences between the surface observations and the radiosonde observations obtained in the free atmosphere at the observatory's 680-mb pressure altitude. These differences are due primarily to severe ground heating induced by the black lava ground cover, the evaporation of water stored in the lava, and the mountain-induced upslope circulation that usually prevails during the day. As a result, the surface observations had to be included as part of the vertical profiles for computing sky radiances. This was done by linear interpolation between some radiosonde "tie on" level values and the surface values. The tie on level was taken as the level that resulted in the minimum r.m.s. difference, for all channels, between the observed sky radiances and those computed for each tie on level using the model adjustment values k_o and k_1. The tie on levels are given in table 2.

E. The Theoretical Transmittance Model

The transmittance model to be used for interpreting the Nimbus E ITPR data has been formulated by Davis (1972) from the technique outlined by Godson (1963). In the Godson technique, the transmittance for a given spectral channel is expressed in terms of a function that represents a combination of the regular and random band models. The model parameters are determined from CO_2 and H_2O transmittances obtained by direct line-by-line spectral integrations for homogeneous conditions. The temperature-dependent weighting factors required to convert non-homogeneous paths to equivalent homogeneous paths are based on summaries of line intensities and line half widths for the appropriate spectral intervals. Differences between the atmospheric transmission functions specified by this model and those obtained by "exact" vertical integrations are generally less than 2 percent.

4. RESULTS OF THE MAUNA LOA OBSERVATIONS

Figures 6 to 12 show the total atmospheric transmittance derived from all the solar radiance data and from the sky emission data for sec θ = 1, 2, 4, and 8 (θ = 0°, 60°, 75.5°, 82.8°). The H_2O concentration was computed as the product of the total precipitable water obtained from the conventional data and the appropriate geometric factor for the angle of observation. The CO_2 concentration along the zenith direction was computed assuming a uniform mixture of .031% by volume. As shown, there is generally good relative agreement between the two independent measurements of total atmospheric transmission. The excessive scatter of the transmission data in the window channel (fig. 6) is due to the fact that observed radiances usually are far out of range of the 0 to 100°C target radiances used to calibrate the data. Consequently, small errors in the calibration slope induced, for example, by small variations of detector temperature will cause errors in the calibrated radiance. The magnitude of these errors is proportional to the deviation of the target temperature from the mid-point of the calibration range. In fact, some of the emission data of channel 2 was disregarded because of negative radiances that resulted from this calibration problem. Some of the scatter also is due to errors in conventional observations of atmospheric water vapor concentration.

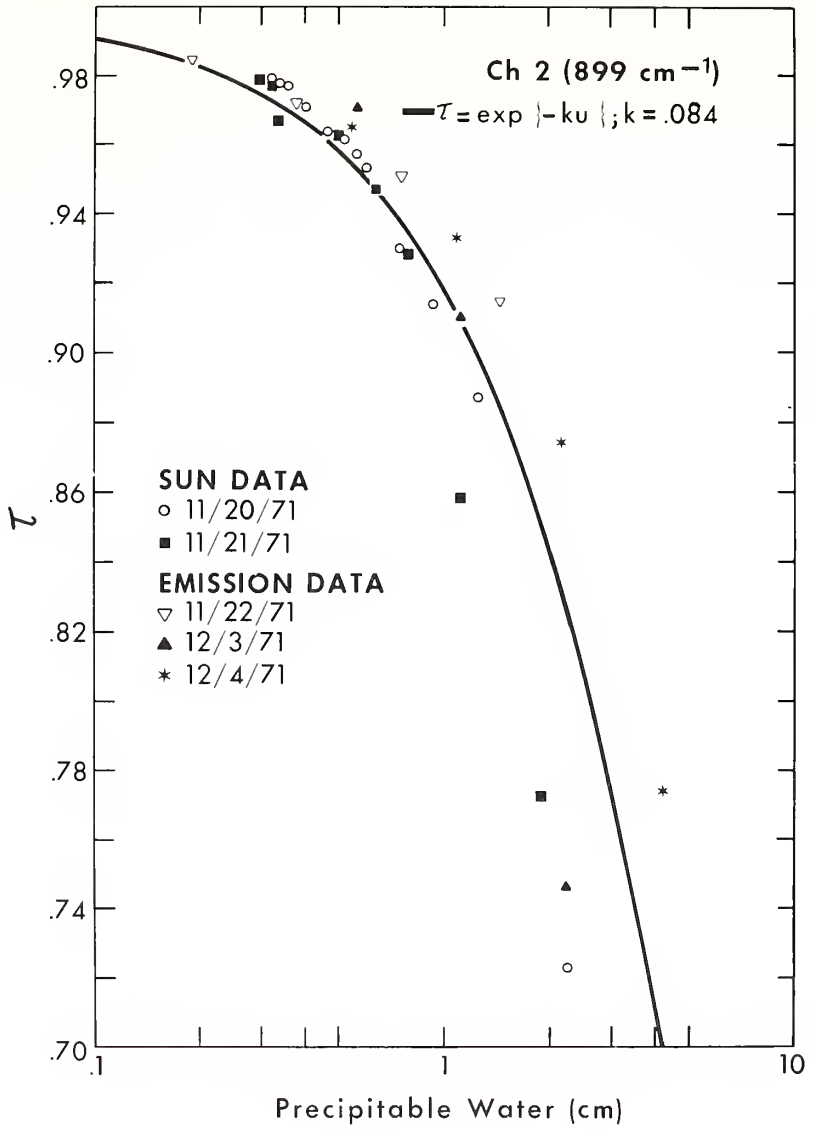

Figure 6.--Transmittance in the 11-μm window region measured by ITPR channel 2. H_2O concentration in precipitable centimeters (pr.cm).

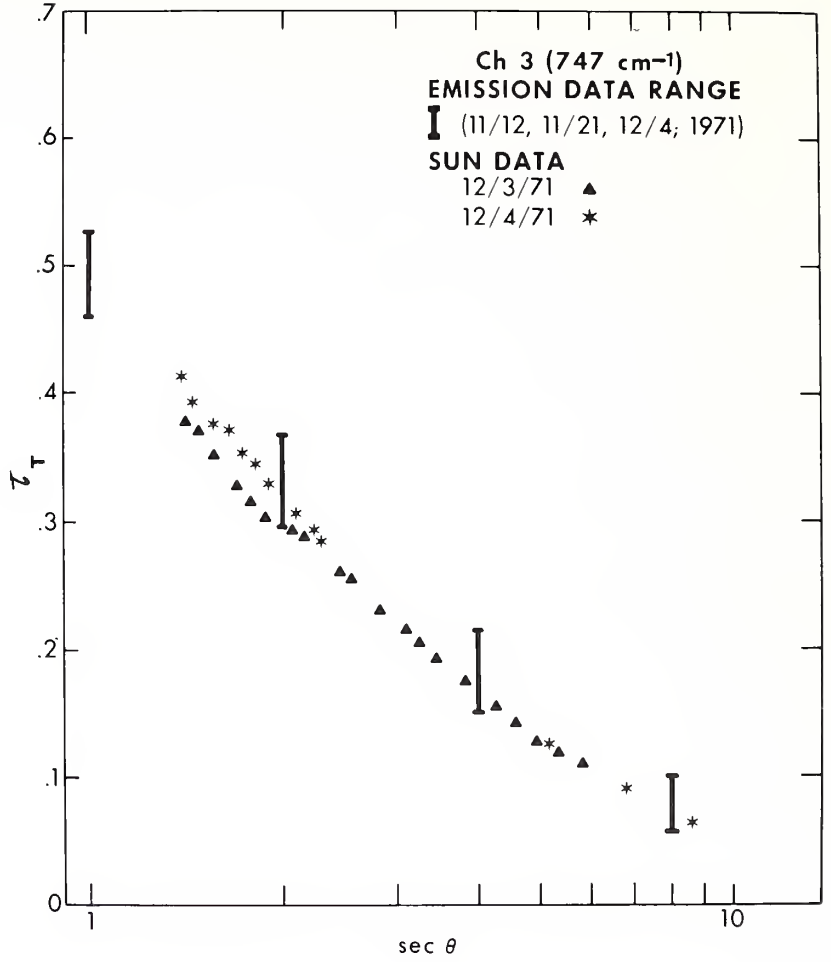

Figure 7.--Total transmittance inferred from ITPR channel 3 measurements.

The calibration problems of channel 2 do not exist for channels 3, 4, and 7. For channels 3 and 4 (fig. 7 and 8) the total transmittances are plotted against the sec θ, since absorption is due to both CO_2 and H_2O. The wide range of the emission data shown here is due to the large difference in H_2O concentration between November 12 and December 1, 3, or 4 (see table 2). One interesting feature in figure 7 is the apparent change in the stratification of the atmosphere between the sec θ values of 1.9 and 2.1 on December 3. This relative drop in transmittance probably was due to the presence of thin cirrus cloud overhead, which is hard to detect visually at high sun. Aside from this feature, excellent relative agreement between the various observation days was obtained for both channels 3 and 4.

To isolate CO_2 components of total absorption in channels 3 and 4, the CO_2 transmittance was estimated by dividing the observed total transmittance by the theoretical H_2O transmittance. The results are displayed in figures 9 and 10. For channel 4 (fig. 9) there is excellent agreement between the CO_2 transmittance estimated from the solar observations, sky emission observations, and those predicted by the theoretical model. For channel 3 (fig. 10), however, the agreement is quite poor. The agreement between the CO_2 transmittances derived from the sun measurements and the emission measurements appears to be poorer than the agreement between the corresponding values of total transmittance (fig. 7); this indicates that the theoretical water vapor transmittances are in error. To verify this, the total transmittances were re-derived from the sky radiances by assuming the model transmittances for CO_2 to be correct; that is, k_o and k_1 were derived for the H_2O transmittance model. Then the total transmittance values obtained from both the sun and emission radiance observations were derived by the theoretical CO_2 values to obtain observational estimates of the H_2O transmittance. The resultant transmittance values derived from the sun and emission observations are shown in figure 11 together with the curve predicted from the theoretical model. Here there is excellent agreement between the sun- and sky-emission data, but drastic disagreement of both with the theoretical estimate. Thus, it is concluded that the model for water vapor transmittance for channel 3 is in error and some parameter adjustment is necessary.

Figure 12 shows the results obtained for the water vapor channel. As shown, there is good agreement of both the sun- and sky-emission data with the theoretical model. The small degree of bias between theory and observations for H_2O concentrations between 0.5 to 1.5 precipitable centimeters (pr.cm.) is probably within the error of estimation of H_2O concentration.

5. CONCLUSION AND ADDITIONAL CONSIDERATIONS

The Mauna Loa experiment has shown that ground-based sun and sky radiance observations with a satellite-prototype sounder can be used to determine atmospheric transmission for its spectral intervals of observation. Such observations can be used in conjunction with theoretical values or with empirical data to construct accurate analytical models of atmospheric transmission functions for application to the spacecraft soundings.

Reliable radiances could not be observed at Mauna Loa for the atmospheric window spectral regions because the observed radiances were outside the

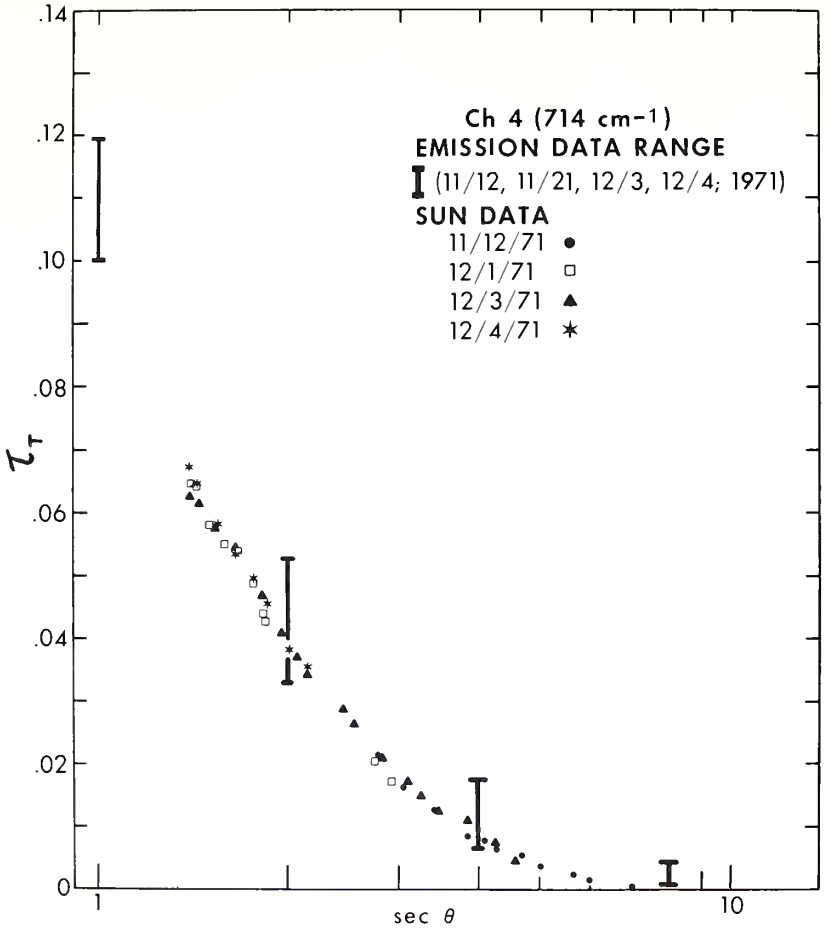

Figure 8.--Total transmittance inferred from ITPR channel 4 measurements.

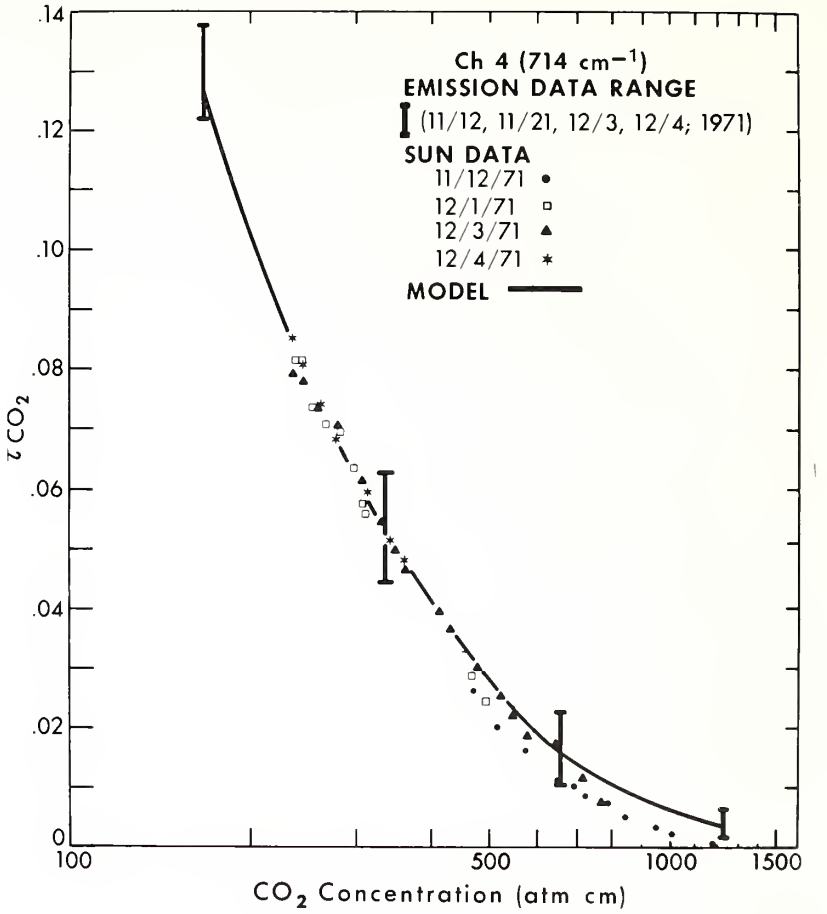

Figure 9.--Derived CO_2 transmittance for ITPR channel 4.

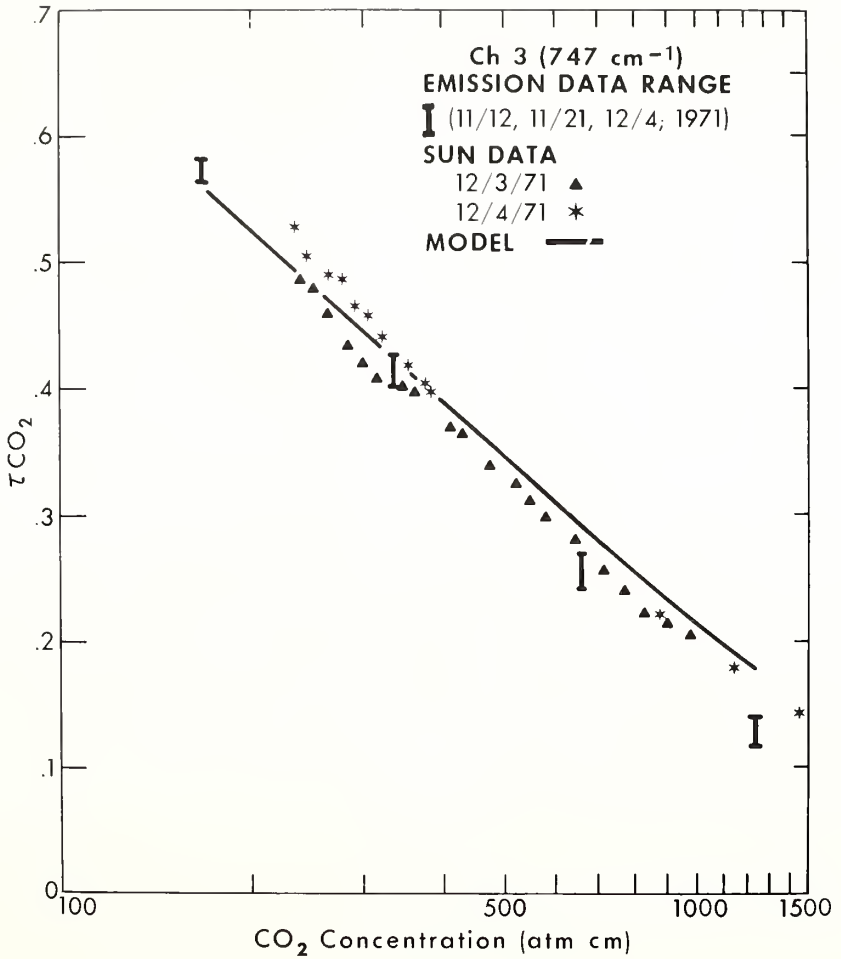

Figure 10.--Derived CO_2 transmittance for ITPR channel 3.

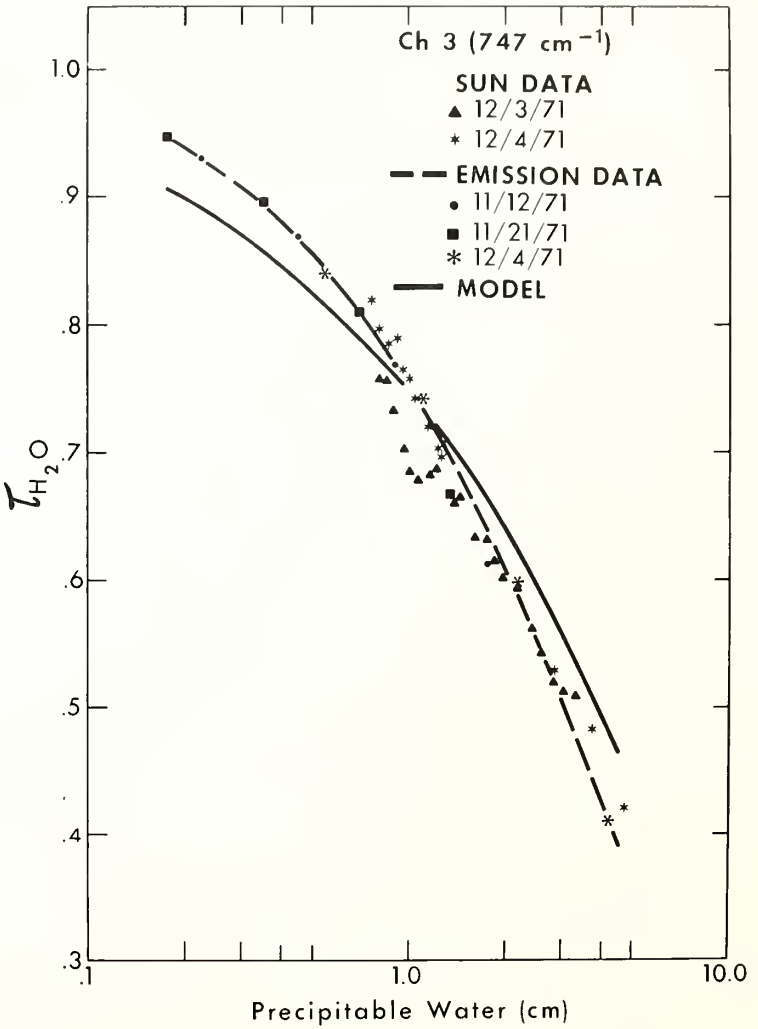

Figure 11.--Derived H_2O transmittance for ITPR channel 3.

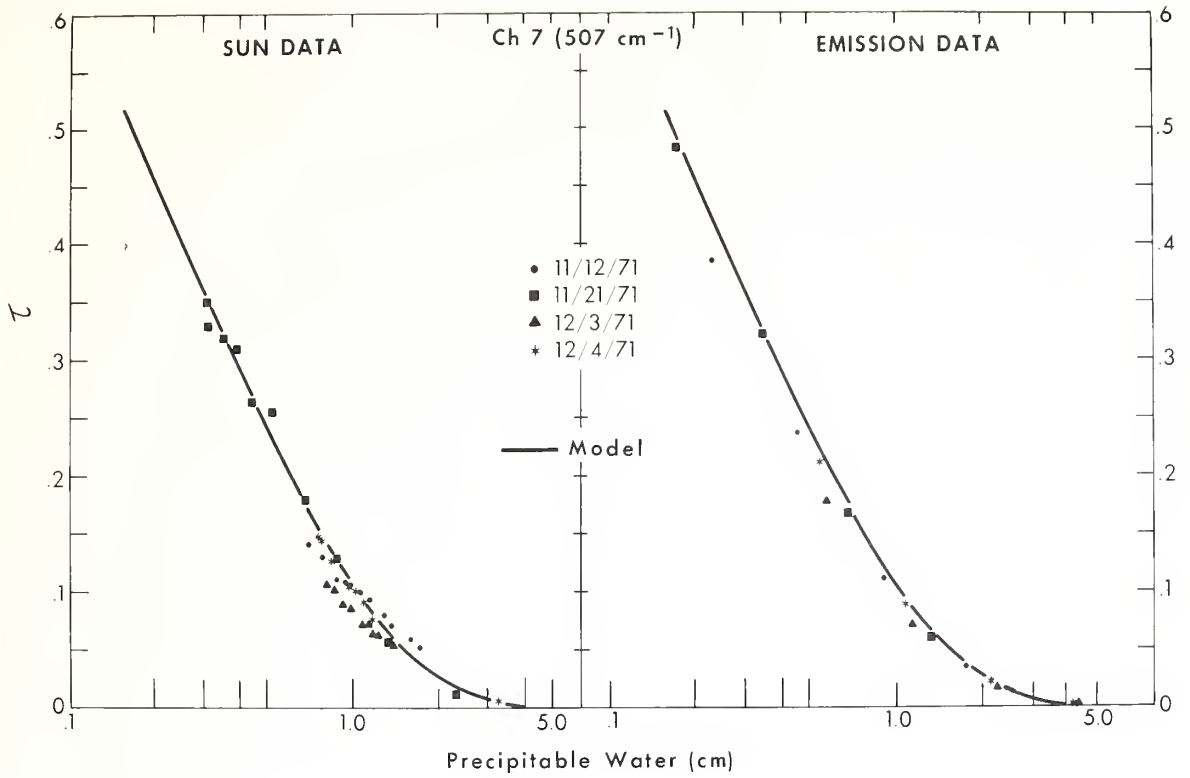

Figure 12.--H_2O transmittance inferred from ITPR channel 7 measurements.

dynamic range of these channels. Instrument gain reduction and a larger calibration blackbody temperature range should overcome this difficulty.

ACKNOWLEDGEMENTS

This experiment was funded by the National Aeronautics and Space Administration. The authors convey their thanks to Harry Press of NASA for his support.

We also thank J. Kapsch, F. Mignardi and J. Fischer for their technical support given in arranging and conducting the Mauna Loa Experiment. P. Pellegrino of this Laboratory deserves recognition for taking and reducing the supporting radiosonde observations. We also thank him, L. Mannello, W. Kohri and R. Ryan for their assistance in the reduction and analysis of the radiance data. Our special thanks go to R. Pueschel and his staff at the Mauna Loa Observatory and Mr. Busniewski and his staff at the Hilo Weather Station for their cooperation and warm hospitality.

REFERENCES

Davis, Paul A., "Transmittance Representation for Application for ITPR Measurements," Final Report, NOAA Contract 2-35136, SRI Project 1385, Stanford Research Institute, Menlo Park, California, 1972, 45 pp.

Godson, Warren L., "Infrared Transmission by Water Vapor," Archiv. für Meteorologie, Geophysik, und Bioklimatologie, Series B. Band 12, Heft 2, 1963, pp. 196-223.

Thekaekara, Matthew P., Drummond, Andrew J., Murcray, D. G., Gast, P. R., Laue, E. G., Willson, R. C., "Solar Electromagnetic Radiation," NASA Report SP-8005, GSFC, Greenbelt, Maryland, May 1971, 33 pp.

☆ U. S. GOVERNMENT PRINTING OFFICE :1972—511-319/84

(Continued from inside front cover)

NESS 57. Table of Scattering Function of Infrared Radiation for Water Clouds, Giichi Yamamoto, Masayuki Tanaka, and Shoji Asano, April 1971. (COM-71-50312)

NESS 58. The Airborne ITPR Brassboard Experiment, W. L. Smith, D.T. Hilleary, E. C. Baldwin, W. Jacob, H. Jacobowitz, G. Nelson, S. Soules, D. Q. Wark, March 1972.

NESS 59. Temperature Sounding From Satellites, S. Fritz, D. Q. Wark, H. E. Fleming, W. L. Smith, H.Jacobowitz, D. T. Hilleary, and J. C. Alishouse, July 1972.

NESS 60. Satellite Measurements of Aerosol Backscattered Radiation From the Nimbus F Earth Radiation Budget Experiment, H. Jacobowitz, W. L. Smith, and A. J. Drummond, August 1972.

PENN STATE UNIVERSITY LIBRARIES
A00007201831L